DOE/PC/95231-18
DIST. CATEGORY UC-112
UTSI-98-04

TECHNICAL PROGRESS REPORT
FOR
UTSI/CFFF MHD PROGRAM COMPLETION
AND RELATED ACTIVITY

For The Period
October 1, 1998 - December 31, 1998

January 1999

Work Performed Under Contract No. DE-AC22-95PC95231

Prepared for:
The United States Department of Energy

Prepared by:
The University of Tennessee
Space Institute
Energy Conversion Research and Development Programs

TABLE OF CONTENTS

LIST OF FIGURES

Page

LIST OF TABLES

EXECUTIVE SUMMARY

Maintenance of the DOE CFFF facility was suspended, due to a stop work order issued in September 1998. Property accounting actions were continued on a minimum basis with university funding. No work was done on the environmental management and environmental restoration for the facility.

Continued progress is reported on the five (5) high temperature superconductivity projects under Task 6. A cooperative group has been formed to facilitate the development of chemical processes for the manufacture of HTS superconductor wire. The group includes EURUS Technologies, Incorporated, Sandia National Laboratory, Clemson University, University of Houston and the National Magnet Laboratory. The ac loss project continues laboratory work in an effort to determine the optimum configuration for multiple conductor cables to minimize the ac loss. The cost/performance analysis concentrated on addressing comments on the draft Topical Report on the life cycle cost analysis of coated conductor manufacture by electron beam and PLD. Work on diagnostics for real time process control reported includes surface smoothness measurement by scatterometry, Raman scattering for real time determination of crystalline structure and oxygen content and atomic absorption measurements for control of stoichiometry in MOCVD deposition of YBCO.

TASK 1 - FACILITY MAINTENANCE AND PROPERTY MANAGEMENT

Work on maintenance of the CFFF was suspended during September in accordance with DOE instructions.

TASK 2 – REPORTING AND ARCHIVING

DOE issued a Stop Work Order for CFFF maintenance in September 1998.

October, November and December Monthly Status Reports were submitted.

The July-September 1998 Quarterly Technical Progress Report and Key Personnel Staffing Report were submitted.

Received and processed Modification A004 to incrementally fund and allocate $50K to Tasks 1-5.

Received and processed Modification No. 05 to incorporate the following items into the contractors acquired government property listing:

Lindbergh Tube Furnace
Programmable Controls for Tube Furnace

TASK 3 - SITE ENVIRONMENTAL COMPLIANCE AND REMEDIATION

DOE suspended Work on site environmental compliance and remediation.

TASK 4 - SITE REACTIVATION

No work was scheduled or performed.

TASK 5 - DISASSEMBLY AND DISMANTLEMENT (D&D) OF THE CFFF

No work was scheduled or performed.

TASK 6 - ADVANCED TECHNOLOGY, RESEARCH, DEVELOPMENT AND ENGINEERING FOR OTHER FEDERAL OR DOE PROGRAMS

Subtask 6.02 - Evaluation of Methods for Application of Epitaxial Buffer and Superconductor Layers

During the report period of October 1, 1998 to December 31, 1998, the following progress was made on the above project.

- The bench scale dip-coating unit was modified so that a tape supplied from a feeder spool can be coated. Using the salvaged parts, a temporary system capable of coating about 10-12 inches long tape has been put together. It will be tested using a dummy (unrolled) metal tape that is easily wetted by the $LaAlO_3$ precursor solution. In the future, necessary modifications will be made to this temporary system that may also incorporate a receiving spool for the coated/dried tape and be more presentable.

- To thermally treat the buffer and YBCO precursor material coated tapes/samples, a high-temperature furnace system has been designed and assembled. It includes a programmable

control to provide correct time-temperature profile for processing YBCO films. In the center of the furnace, a specially designed quartz tube insert is housed in which the coated samples are placed and then thermally treated for predetermined time at the desired temperature and under desired gas atmosphere. The assembling of this system is almost complete. Because of inadequate power voltage (208 volts instead of 240 volts), at present, it is difficult to reach temperature beyond 1200°C even though the furnace is capable of going up to 1500°C. As a result, a step-up transformer will be required to increase the input power voltage. The furnace is about 36 inches long and can handle samples as long as 12 inches long and maintain them uniformly at the desired high temperature.

- UTSI representatives (Drs. J. Muehlhauser and A. Sheth) attended an exploratory meeting organized by EURUS Technologies, Incorporated and the National High Field Magnet Laboratory. This meeting was organized to form a working group and several sub-groups pursuing research and development work in the area of solution-growth based techniques (e.g. sol-gel, MOD, CSD). As a follow-up to this meeting, a one-page write-up describing objectives, available facilities, approach and potential partners for the UTSI's program on Coated Conductor Development was prepared. This write-up will be distributed to the attendees for their comments at the second meeting of this group, which is tentatively planned at present to take place during the January 1999 Wire Workshop to be held in Cocoa Beach, Florida.

- The technical paper discussing UTSI's work on process evaluation was revised to include the editor and peer reviewers' comments. The revised paper has been now submitted to the editor of the Journal of Applied Superconductivity for publication. However, we still do not have Doe's official release to publish it.

- Similarly, the poster paper presented at the ASC '98 Conference describing UTSI's bench scale sol-gel related work was revised to incorporate the peer reviewer's comments for publication in the IEEE Transactions on Applied Superconductivity.

Subtask 6.03 Coated Conductor Development and Program Management

Informal coordination continued with members of the Advisory Committee related to revisions in the Draft Research and Development Roadmap to Achieve Electrical Wire Advancements from Superconducting Coatings. The draft topical report prepared under Subtask 6.05 was forwarded to Advisory Committee members for review and comment.

Subtask 6.04 Optimum Coated Conductor

The setup for measuring critical currents in superconductors was described more completely in the previous quarterly. Basically, a strip of superconductor tape up to a meter in length can be placed in a Styrofoam box and immersed in liquid nitrogen. A nanovoltmeter is used to measure the voltage drop along the superconducting tape using a 1-microvolt per cm standard for critical current.

Initial tests of the setup with ordinary #12 copper wire and a ballast resistor in the circuit demonstrated that the resistance of the copper wire could easily be measured over short sections of the wire with the nanovoltmeter. Good linearity of the results was indicated for currents up to 20 amps. The tests also indicated that the ballast resistor was not required and that the resistance of the circuit hook up wires, which were #12 solid and stranded wires, was sufficient for the power supply to operate satisfactorily. The next step was to measure the resistance of the superconductor tape in a normal condition, *i.e.* at room temperature. Four voltage leads were soldered to the tape: one lead near each end, one lead at the half-length position and one lead at the quarter length position. Results obtained were less than satisfactory in that measurement

errors were apparently introduced. The errors were either procedural errors associated with not properly zeroing the nanovoltmeter when changing range scales or problems with the solder joints where the lead wires were soldered to the superconducting tape.

A current shunt in the circuit is used to measure the current (rather than relying on the power supply meter) for increased accuracy at the low current, low voltage condition of the power supply. It was necessary to use the nanovoltmeter to alternately measure the voltage drop across the current shunt and the tape under test and this involved range changes between the measurements. A more sensitive portable voltmeter than the one available should be capable of reading the voltage drop across the current shunt to a satisfactory accuracy and allow the nanovoltmeter to be dedicated to the tape measurement alone. To evaluate solder joints concerns other tape samples will be tested independently. That is to test a sample before and after soldering leads to it to ascertain if good joints are obtained and if the soldering can thermally degrade the superconductor. The original solder joints were made with a low wattage iron to minimize the heat transferred to the superconductor tape. Perhaps, due to the high thermal conductivity of the silver, cold solder joints resulted and a higher soldering temperature is required. In retrospect, it is believed that the precaution to minimize the tape temperature was probably unfounded as the soldering temperature is well below the normal temperature used in processing the BSCCO tape.

Subtask 6.05 Cost/ Performance Analyses of Potential Manufacturing Processes

The major activities this quarter were in revising the draft topical report, "Life Cycle Cost Study for Coated Conductor Manufacture by Electron Beam and Pulsed Laser Deposition Systems". During the quarter, the revisions discussed were completed and the draft report forwarded to DOE/FETC for approval for publication.

The most significant revision was in the process of ejection of YBCO from the target to the substrate. The original draft study treated this effect as vaporization and used the same efficiency of material utilization as used for electron beam vaporization, 10.6%. Further literature review revealed that vaporization, even with a pulsed laser, does not produce a stoichiometric YBCO flux at the substrate. Instead, PLD depends upon a particulate flux, which is stoichiometric, and results from application of the correct energy density at the target. If the energy density is too low, non-stoichiometric vaporization results. If it is too high, larger particles are contained in the beam and the correct crystalline structure does not result on the substrate. The beam particle distribution can be approximated by a $\cos^{12}\theta$ function in both directions, where θ is the half angle suspended from the point of laser impact on the target to the substrate. This analysis assumes that the deposition rate variation is acceptable using $\theta = \pm 20°$ in the direction of tape movement. However, in the direction across the tape, a variation of -10% thickness of the tapes is chosen, which corresponds to a $\theta = \pm 7.6°$ beam width. For the 50 cm horizontal deposition region, this corresponds to an 18.3 cm vertical span or a total deposition area of 50 cm $\times$ 18.3 cm = 915 cm^2. The efficiency of beam material utilization can be calculated based on these choices as,

$$\eta = \frac{\int_{-20°}^{+20°} \cos^{12}\theta_x \int_{-7.6}^{+7.6} \cos^{12}\theta_y d\theta_y}{\int_{-90}^{90} \cos^{12}\theta_x d\theta_x \int_{-90}^{90} \cos^{12}\theta_y d\theta_y}$$

However, since the PLD process depends on a relatively smooth surface and for other practical reasons, only about 70% of the YBCO in the target can be used. Thus, the material utilization efficiency becomes $0.229 \times 0.70 = 0.16$.

Use of this material utilization efficiency results in reduced material costs that tend to narrow the cost gap between electron beam and PLD somewhat. The material costs for this study are shown in Table 6.05-1.

Table 6.05-1 Consumable Cost for Assumed Production

		E-Beam	PLD
Materials	**Unit Cost, $**	**Annual Cost, $**	**Annual Cost, $**
Nickel	38.27/kg	2,330,000	2,330,000
Yttrium	345/kg	2.049,000	
Barium	124/kg	2,300,000	
Copper	41/kg	523,560	
Cerium	394/kg	79,082	79,082
YSZ	1,298/kg	246,865	246,865
YBCO	300/kg		8,836,425
Gases, Supplies		500,000	500,000
Subtotal Materials, $/yr.		**8,028,507**	**11,992,372**

Calculation of the capital costs for the PLD process depends critically on the number of lasers and vacuum chambers required. The energy required to eject a beam of solid particulate in the regime needed for this application appears to be higher than the energy required for vaporization. Laboratory scale measurements indicate 1.14×10^{-5} grams/Joule of energy. An assumption has been made for the base case that slightly more than 3 times this energy efficiency will be possible in a system designed for commercial service, for example, 3.75 grams/Joule. This permits meeting the production rate with 80 excimer lasers operating at 200 pulses/second, 1 Joule/pulse. This assumption is examined in a sensitivity analysis in the revised report. Thus, no changes are made in the capital cost estimate in the original report.

With the revised consumable costs, the cost of production is summarized in Table 6.05-2. This table shows that the production cost with PLD, even with the improved material utilization efficiency, is almost twice that for an electron beam process. Several comments were received suggesting that other, cheaper lasers be used instead of excimer lasers. Consultation with PLD experts found no support for this idea for depositing YBCO stoichiometrically, although single elements have been successfully deposited by longer wavelength lasers. Also, a long wavelength laser can be used to vaporize the precursors individually, but this makes no sense economically. In addition, comments were received that a single wide sheet of superconductor should be manufactured, then sliced into the desired width. This would enable lower cost tape handling equipment if it can be done successfully.

Table 6.05-2 Production Costs Summary

	Electron Beam	PLD
Total Capital Cost, $	30,950,110	88,185,588
Annual Capital Charges @ 24.7%	7,644,677	21,781,840
Maintenance @ 10% of Capital Cost	3,095,011	8,818,559
Materials Costs, $/yr.	8,028,507	11,992,372
Labor, $/yr.	9,013,486	9,974,664
Electricity, Other Utilities, $/yr.	3,000,000	3,000,000
Total Annual Cost, $	30,781,681	55,567,488
Annual Production, m	18,000,000	18,000,000
Critical Current*, A	400/40	400/40
Cost, $/m	1.71	3.09
Cost*, $/kA-m	4.28/42.75	7.72/77.18

**First number is for $J_c = 10^6$ A/cm^2, second is for $J_c = 10^5$ A/cm^2.*

Subtask 6.06 Development of Real Time Process Control Using In Situ Diagnostics

Optical Scatterometry

Work during this quarter concentrated on developing hardware and software to allow the Finish Measurement System to make scatter measurements over sample areas. This project was undertaken to best serve the needs of researchers developing HTSC substrates that require surface roughness characterization of substrates and layers.

The FMS is primarily a point measurement device. When used for the intended purpose of product or process monitoring, the product is moved through the FMS measurement point and the FMS provides a continuous measurement of the product quality. Product quality may be presented in a variety of ways by the FMS dependent on operational settings. Possibilities include TIS (Total Integrated Scatter), RMS surface roughness (1 and 2 – D models with adjustable spatial frequency limits), BRDF (bi-directional reflection distribution function), and a general purpose linear combination function of the scatter detectors. The choice of data presentation depends on measurement requirements.

For process monitoring, the linear combination function is the best choice. The function is simply a weighted sum of the voltages measured by the four available detectors. This value is converted to an analog value that is output by the FMS and updated at maximum frequency of 500 Hz. Also output are high and low signals indicating whether the computed function is outside the range set by user adjustable upper and lower limits. The combination of flexible output function, rapid data rate, and adjustable range checking make this mode ideal for process monitoring.

The other modes can also be used for process monitoring but are less flexible, require complex communication with the FMS, and cannot be updated as rapidly. TIS and RMS surface roughness each provide a single number derived from the available detector measurements (up to four) and model parameters using internal FMS algorithms. BRDF provides the most complete data of all the modes giving a gain and offset corrected value scaled to BRDF for each of the detectors. Due to the greater amount of data transferred, BRDF measurements are the slowest.

As stated, to make measurements of any type at more than a single spot, provision must be made to move the sample. To allow for area surveys of samples, scanning hardware and software were completed and added to the FMS making automated precision positioning of samples possible. The scanning hardware was based on two micrometer/stepper motor controlled linear translation stages stacked and mounted at right angles to each other. The scanning hardware thus provided two axes (x and y) of translation with a travel of 2 inches and a minimum position resolution of 0.000125 therefore providing approximately 10^7 addressable locations per cm^2. Maximum translation speed is about 250 steps/sec thus requiring 1.1 hours scanning time per cm^2 at maximum resolution. The stepper motors limit the maximum scanning speed. Software control of the translation stages was accomplished with a LabVIEW™ instrument and allowed arbitrary positioning of the stages at settable translation rates.

Software for FMS control and scatter data acquisition was integrated with the LabVIEW™ scanning software allowing area scans of samples to be acquired. The requirements of FMS software control and acquiring data from the FMS limits scanning speed currently to approximately 10 samples/sec speed far below the limit imposed by the scanning hardware. The limit is due primarily to the speed of the serial FMS communication link but FMS hardware setup and operational regimes contribute to the reduction. Software options allow for stepping in large increments (multiples of the minimum step size) to allow coverage of larger regions in reasonable times.

The FMS scatterometer was reconfigured for direct RMS roughness measurements using the supplied algorithms internal to the FMS PC software. Reconfiguring was required because

internal algorithms are substantially limited in scope primarily due to the technique for handling the polarization factor Q. This parameter incorporates several effects of material properties (as opposed to surface shape) on light scatter and can be directly calculated using standard correlations that reduce to Fresnel reflectance equations for the specular reflectance direction. Under the appropriate conditions (s-polarized wave, plane of incidence of scatter, highly reflective (*i.e.,* smooth) surfaces), the sample specular reflectance is a good approximation of Q. FMS PC software makes use of this approximation and thus requires an optical configuration of the FMS that allows measurement of the specular reflection from the sample.

Direct measurements of surface roughness were made on RABiTS nickel strips provided by ORNL and EURUS using the FMS, FMS PC Software, and standard procedures provided in the FMS operations manual. Results obtained were inconsistent and the FMS scatterometer frequently reported out of range conditions. Deficiencies in the FMS PC software and the operating procedures are hypothesized to be causing the difficulties. Discussions with the manufacturer are on going to develop appropriate procedures and corrections.

Measurements continued during the quarter on samples to characterize the ability of scatterometry to detect defects and anomalies. Microscopy was used to identify and locate surface imperfections in various samples and these imperfections were scanned with the scatterometer. The FMS was configured to measure scatter at (66.5°, 0°), (0°, 180°), (30° and (45°,180°) with incident light at (66.5,180°) where the notation is (altitude angle, azimuth angle). Thus the detector at (66.5°, 0°) measured the specular reflection while the other detectors measured scatter at spatial frequencies of 1.369, 1.755, and 2.424 μm^{-1}, respectively. Primarily linear features as small as 0.0025 mm in width were easily detectable as variations of the BRDF as the features were scanned through the measurement beam. Features only 0.0001 inches across showed increases in BRDF of up to 98% with attendant reflectance decreases of 10%, making such anomalies easily detectable.

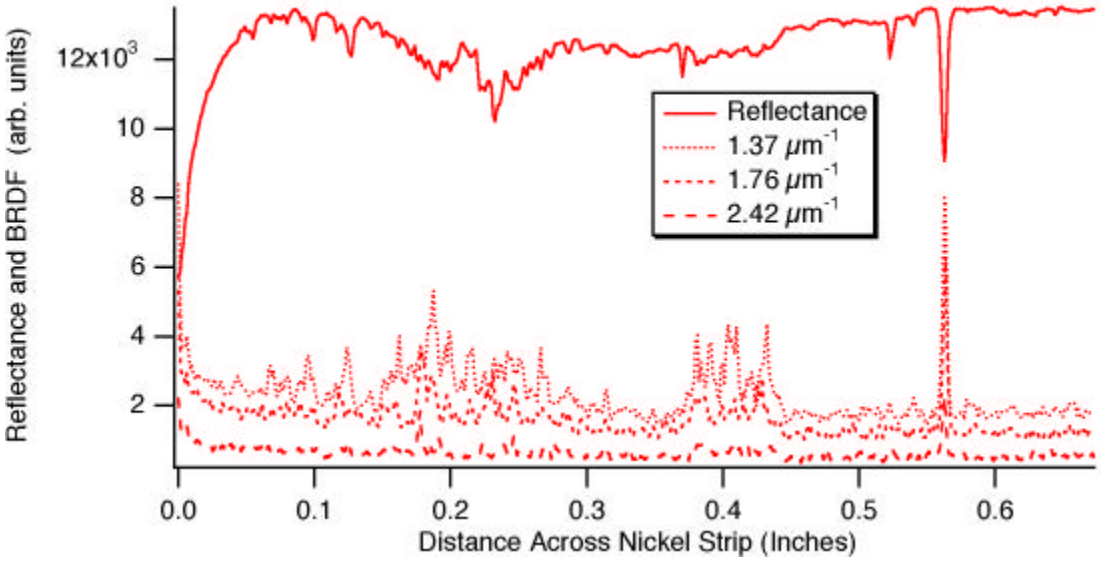

Figure 6.06-1. Variation in Reflectance and Scatter of as-rolled Ni RABiTS Sample.

An example of the variation in the FMS signals due to defects is given in Figure 6.06-1. This figure shows the reflectance and BRDFs measured along the rolling direction of an as-rolled Ni RABiTS sample. The curves show the general complementarity between reflectance and BRDF and the similarity among the BRDFs. This particular sample exhibited a small width defect (0.01 in) at about 0.56 in. which increases sample scatter by more than a factor of four. Also

identifiable in the profiles is a long feature starting at about 0.1 in. and extending to 0.45 in. This feature is primarily a linear feature aligned with the rolling direction.

A series of area scans were made using the scanning system. The FMS detectors were configured as described providing measurements of the specular reflection and scatter at spatial frequencies of 1.369, 1.755, and 2.424 μm^{-1} respectively. To date 22 scans have been completed on an as-rolled Ni RABiTS sample as well as four scans on two annealed RABiTS samples.

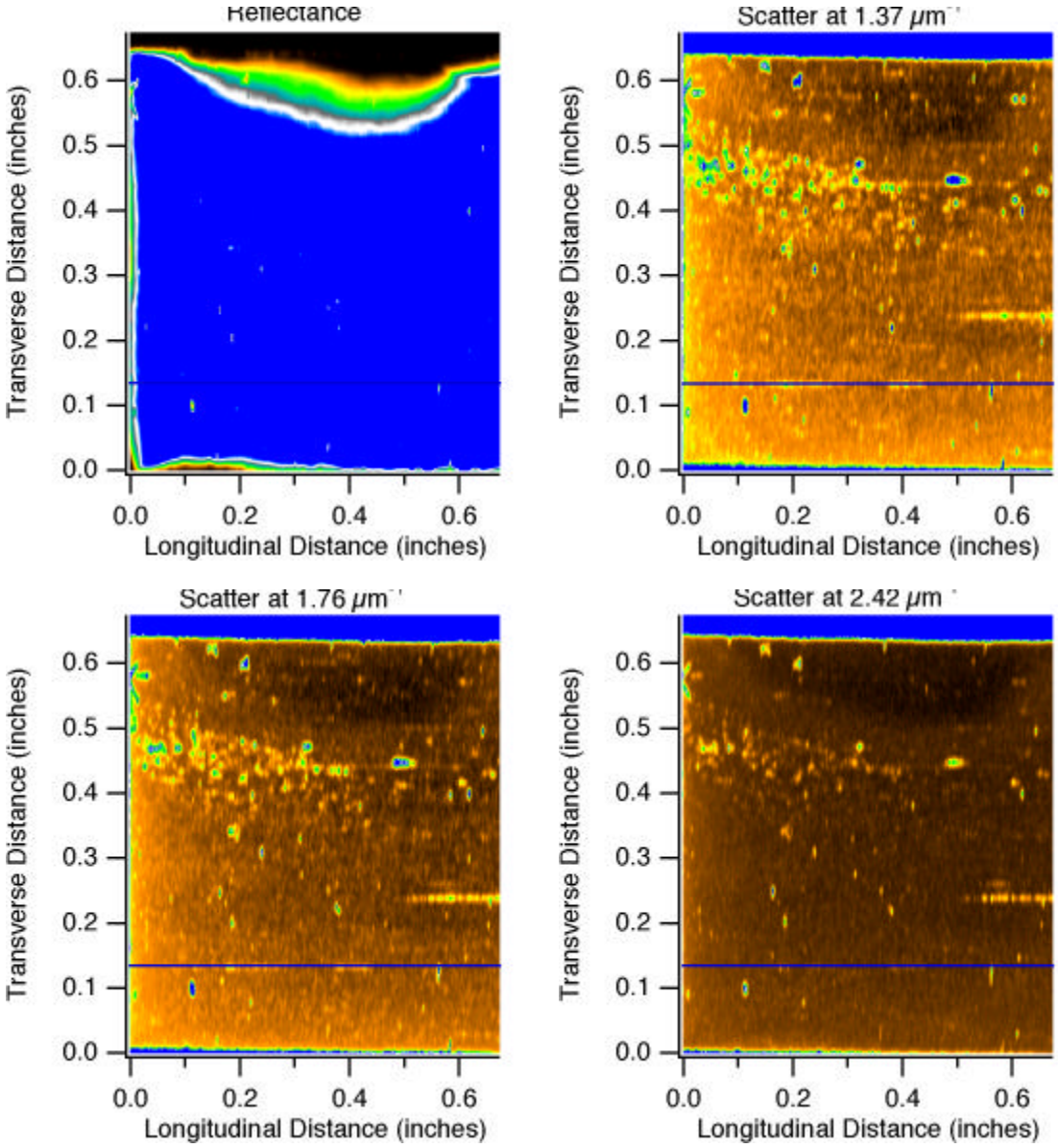

Figure 6.06-2 Reflectance and Scatter of as-rolled Ni RABiTS Sample.

Examples of the scans are given in Figure 6.06-2. The scans on the as-rolled Ni samples ranged in size from 0.0025×0.00375 in. (20×30 steps of 0.000125 in.) to 0.9×0.675 in. (360×270 steps of 0.0025 in.). Thus, the images ranged from small regions at high resolution to images covering the entire sample but with a coarse resolution. The images show the surface to contain many

small linear features (aligned with the rolling direction) as well as circular features. Some high scatter features have scatter intensities of up to 100 times greater than the average background scatter levels. Features as small as 0.001 in. are observable in the scans. In general, high scatter regions correlate well among the three off-axis detectors as well as with decreases in sample reflectivity as measured by detector 1. However, anomalies exist (variations in the amount of off-axis scatter at the different angles and reflectivity changes without attendant off-axis scatter) which may allow the features to be categorized.

All samples scanned to date have shown substantial mechanical deformation. The effect of the deformation is most visible in the measured reflectance and appears as dramatic reductions in reflectance over large regions (see the top of reflectance image of Figure 6.06-2). The deformation is consistent with what could be expected of thin foils that have been flexed during handling, cutting, or other preparation. Due to the deformation the local surface may be substantially tilted (up to several degrees) compared to the mean sample surface.

Such tilting, if great enough, introduces error into the Q parameter that must be known for conversion of scatter measurements to roughness quantities. For highly polished metal samples such as RABiTS substrates, Q is simply the reflectivity of the sample and is easily measured with a detector intercepting the specularly reflected beam. However, surface tilting, if large enough, will introduce errors into this measurement due to finite angular size of the reflectivity detector. Various approaches are being considered to eliminate this problem (better mounting, measurement over smaller regions, numerical extrapolation, detector modifications, etc.) This problem is not expected to exist in a manufacturing installation as the sample deformations all appear to be the result of small sample size and handling.

Film Thickness Measurement

Principally, research was conducted into the two primary methods used in film thickness measurement – reflectometry and ellipsometry and their variants. While spectroscopic ellipsometry appears the best choice for measurements on superconducting thin film stacks, it does have shortcomings. Difficulties with measurement on thin metallic layers, large spot size, lower precision and reproducibility are some of the problems with spectroscopic ellipsometry.

Samples of $LaAlO_3$ on $LaAlO_3$ and $LaAlO_3$ on $SrTiO_3$ prepared via sol gel were sent to Filmetrics, a company specializing in normal incidence spectral reflection spectrophotometry, for a test measurement of thickness using their spectral reflectometer. Preliminary results were received providing thicknesses of 151.9 nm for the LAO/LAO sample and 187.9 nm LAO/STO.

A new acoustical thickness measurement technique, picosecond ultrasonics, is also being investigated. This technique has the advantage of being able to measure film thicknesses of complex metal film stacks. The method is noncontact and nondestructive and can measure six or more layers simultaneously. The concept is simple using pulses of light to generate and detect sound in opaque films. A picosecond laser produces a light pulse on the sample area. The absorption of the laser light causes a very small rise in temperature near the surface of the film. The resulting rapid thermal expansion produces a sound wave that propagates away from the surface at the speed of sound. When the sound wave interferes with a lower layer, the wave is reflected producing an echo that effects the film's reflectivity when the echo reaches the upper surface. The reflectivity change is monitored with a laser. The technique seems to be very robust and well suited for industry where a high level of automation is required.

Another method of measuring film thickness was briefly investigated called Prism Coupling. In this method, a prism is pneumatically controlled to a small distance from the sample. A laser beam then strikes the base of the prism and is normally reflected into a photodetector. At certain discrete "mode angles", photons can tunnel across the air gap into the film and optically propagate through the film causing a drop in the intensity at the detector. This method may not

be applicable to superconducting thin film studies because of its incapability to measure very thin films (<1000 Angstroms.) It can also only measure thickness on single or dual layer film stacks. However, this method does make direct thickness measurements in contrast with ellipsometry techniques for which the data is periodic with film thickness. Prism coupling also measures the index of refraction quickly and accurately. The Metricon Corporation makes devices implementing this method of film metrology.

Data compilation of the several commercial ellipsometers, reflectometers and other thin film measurement devices was completed. This information was compiled to identify current measurement techniques, abilities, and costs helping to identify current availability, suitability to particular needs of the superconductor industry, and typical purchase and implementation costs. Simple laboratory devices have been characterized as well as completely automated systems designed for the semiconductor industry. Several of these commercial devices utilize several different methods to resolve film thickness in multi-layer stacks. Most of these devices also provide information on other characteristics that may be on interest such as surface roughness and homogeneity.

Price estimates of commercial ellipsometers and reflectometers have been extremely difficult to receive. Most companies insist on a demonstration of their product and need process and requirement data to determine system configuration and cost. Since most HTSC process parameters are only vaguely known at this time, cost estimates cannot be made for the more complex instrumentation. Price quotes can be obtained for the smaller, simpler devices designed for laboratory.

Currently there appears to be no completely suitable in situ method for measuring the thickness in complex high-temperature superconductor stacks that contain dielectric or transparent films under a relatively thick opaque or metallic layer. A combination of methods may be required.

Raman Spectroscopy

During the last quarter effort was expended in two areas: continued literature survey and instrumentation improvement via noise count quantification (dark and background), spectrometer calibration, and software development.

Literature Survey

A. Created comprehensive bibliography of articles referring to Raman spectroscopy for thin films and YBCO.

B. Obtained a number of additional articles that had been released in the last six to nine months on this topic and updated bibliography.

C. Reviewed material on commercial Raman systems that might be applicable to this project.

Instrumentation Improvement

A. Dark Count

Ran a series of dark count checks on replacement photomultiplier tube (Hamamatsu R955). Four series of tests, each exceeding 24 hours, indicated that the dark count of the tube averaged between 7-8 counts per second when the tube is cooled to about -30C. This tube replaced a Hamamatsu R928, which had been used earlier to gather data. A series of similar tests were run on that tube before it was replaced showing that tube had a dark count of 3-4 counts per second.

B. Background Count

A background count test to measure the counts from background radiation sources. These sources include room lighting, fields from monitors and power supplies, and scattered light from the Ar laser. The preliminary test showed background counts in excess of 60 per second from these sources with the spectrometer slits set to 0-0-0 (fully closed). The spectrometer was then shielded by draping the spectrometer and the PMT housing with black plastic. This reduced the background counts to 28-30 per second with the spectrometer slits fully closed as above.

C. Spectrometer Calibration

Three series of spectra were taken using a Na source. The doublet at 16961 cm^{-1} - 16978 cm^{-1} were clearly resolved with the proper interval between peaks, although the wavenumbers were shifted approximately +15 cm^{-1}.

Calibration using emission spectra of the Ar^{+} plasma was also performed and compared with published data. Three series of data were taken between wavenumbers 20000 cm^{-1} and 19000 cm^{-1}. The results of these tests showed that the relative wavenumbers corresponded with published data. The relative intensities were not in agreement with published results, nor were they consistent from one set of data to another.

After performing the wavenumber calibration specified in the spectrometer calibration manual, two additional data runs were performed. Initial results showed better agreement with published results of relative intensities. Two more comparison spectra will be run to compare the results with published results.

D. Software

Data acquisition and control for this experiment is being done with LabVIEW™ (v. 4.1) running on a Macintosh II_{fx}. The VI (Virtual Instrument) being used, Raman 4.1 was developed locally. This program does not have the ability to recover data from long experimental runs if the experiment ends abnormally (*i.e.* cancellation by user, power failure, or computer error). Since the data runs for this project are currently very long, exceeding six hours to scan a range of 700 wavenumbers under certain operational regimes, a great amount of time can be wasted in the event of an abnormal termination.

To eliminate this difficulty, the data handling and file management routine of the VI was extensively revised to allow data to be saved in real time, so that experimental results could be recovered from abnormally ended runs. During this revision, some computational overhead not related directly to data gathering and instrumentation control was eliminated.

Atomic Absorption Spectroscopy of MOCVD Precursors

Checkout continued of the experimental apparatus for the feasibility study of Atomic Absorption Spectroscopy (AAS) as a control measurement for the gas flow concentrations of YBCO precursors in the Metalorganic Chemical Vapor Deposition (MOCVD) processing scheme. Vacuum leaks were eliminated to provide capability of maintaining a vacuum of better than 0.3 Torr in the optically accessible precursor vaporization chamber. (A typical MOCVD process vacuum is 1 Torr.) In addition, the spectroscopy system response to the deuterium broad band ultraviolet (UV) light source was evaluated. Initial transmission signal levels were inadequate for AAS at wavelengths below 250 nm, but installation of a different detector and repair of the detector cooler and insulating window improved the capability to wavelengths as short as 215 nm. A noise level check was accomplished and reduction of detected low background was accomplished with improved spectrophotometer sealing and scanning without room lights. Since

MOCVD precursor vaporization is primarily temperature dependent an accurate platinum resistance thermometer was obtained for improved chamber temperature monitoring.

The Atomic Absorption Spectroscopy (AAS) baseline response characteristics were examined for the chamber at atmospheric conditions, vacuum conditions (0.3 Torr) and heated vacuum conditions (300°C, 0.3 Torr). Unfortunately, response changes and window examination indicated a contaminant in the oven had vaporized and condensed on the windows. The windows were cleaned using 0.05 μm alumina polishing powder and a concentrated sulfuric acid-chromium trioxide solution, followed by a water wash, a highly filtered acetone wash, and a highly filtered methanol wipe. Contaminant removal from the oven by thermal vaporization under a trickle purge flow was attempted. Minor contamination continued to occur, and appears to be coming from the internal oven insulation. The window mounting arrangement is being modified to eliminate gas flow from the insulation area to the oven. In addition, heating the windows results in moderate wavelength dependent increases in UV absorption at wavelengths below 290 nm because of changes in sapphire absorption. Steps to account for this baseline change will be implemented in the LabVIEW™ data acquisition and analysis system.

Objectives for next Quarter include obtaining adequate spectral baseline data, then performing AAS scans of the absorption chamber using gases having known UV absorption spectra. This will allow the AAS system operation to be evaluated under desired operating conditions, verify system detection of known absorption wavelengths, and define if single or multiple beam passes are adequate. Scans of precursor samples will be made to identify spectral regions for further focus and finally detailed spectra of the vaporized MOCVD precursors will be obtained to identify absorption lines with potential use for precursor concentration monitoring. If possible, line strength vs. precursor concentration will be measured for a few concentration variations.

Analytical Diagnostics

XRD or Other Analytical Support of External DOE Sponsored HTS Programs

No work requested or performed during this quarter.

XRD or Other Analytical Support of Internal HTS Projects

No work was requested or performed during this quarter except for the substrate texturing (*i.e.* Ni annealing) study.

Ni Annealing Study

Experimental efforts continued aimed at finding avenues to improved texturing of rolled and annealed Ni tapes. The Ni tape used was provided by Plastronic, Inc. through a cooperative agreement and was 99.98% Ni with a 95% rolling reduction to 0.002 inch thickness. Short pieces of tape were annealed in argon, backfilled from a baseline vacuum of 0.2-1 x 10^{-7} Torr, by resistively self-heating the sample by the passage of DC current. This method provides very rapid heating and cooling, precise control, and temperatures to near melting. It was determined that significant texture improvement, in terms of both sharpened cube texture and reduced twinning, can be achieved by removing some material from the surface of the tape through high temperature vacuum evaporation. This pretreatment step normally consisted of a 30 second heating to near melting in high vacuum, prior to argon backfilling and continued annealing at very high temperatures (just below the melting point). Figure 6.06-3 shows data for omega scans about the rolling direction with and without evaporative cleaning. Results from omega scans about the transverse direction and phi scans are also given for evaporatively cleaned samples. Annealing currents were higher for the non-cleaned samples because they were thicker, not having been evaporatively thinned. Removal of a NiO film having (111) orientation is assumed

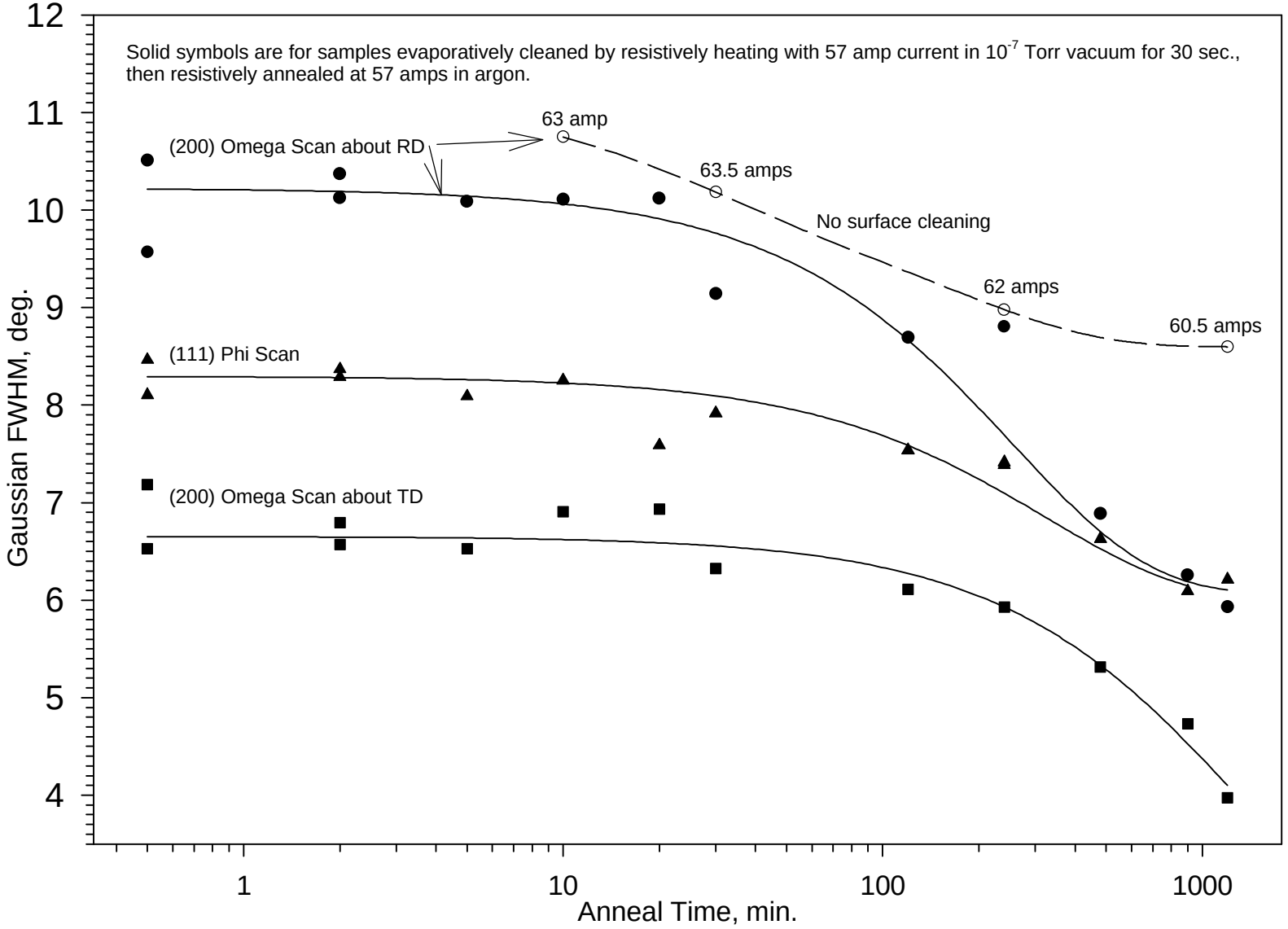

Figure 6.06-3. Comparison of UTSI Anneals of Plastronic "B" Nickel Tape With and Without Surface Evaporative Cleaning

the reason for the texture improvement due to the evaporative cleaning. The data also show the exponential decline of texture sharpness with time.

Figure 6.06-4 shows twin volume percent as a function of anneal time. The evaporative surface pre-treatment greatly reduced twinning for all anneal times. Twinning was eliminated by the long term anneals. It may also be noted that much less twinning occurred with the Plastronic "B" tape, which was otherwise identical to the "A" tape. While most of the "B" tape data followed well a hyperbolically decreasing trend with time, a few points inexplicably showed much less twinning. We have thus far been unable to consistently obtain those lower twinning values. Nevertheless, the "normal" results show that by annealing at very high temperature for short times of up to a few minutes, reasonably low twin volumes and texture sharpness can be obtained. For example, a 30 sec. anneal near melting, following surface cleaning, yields a twin volume of about 4.6%, along with out-of-plane Gaussian FWHM values of 10.2 and 6.6° from scans about the rolling and transverse directions, respectively, and a (111) phi scan FWHM of 8.3°. At these very short times only very shallow grain boundary grooving and no grain internal surface waviness occurs. We believe low twinning and good surface smoothness to be more critical substrate characteristics than extremely sharp cube texture to the end objective of obtaining high HTS critical current densities. Short anneal times translate to rapid throughput and lowered cost of production.

Long duration (20 hr.) anneals yielded out-of-plane FWHM values of about 6° and 4° from scans about the rolling direction and transverse direction, respectively, with a (111) phi scan FWHM of about 6°. Despite achieving very sharp cube texture and very low or zero twinning, negative consequences of long-term very high-temperature annealing are deep grain boundary grooves and a highly pronounced undulating roughness of the grain interiors. This roughness would offset much of the long-term Ni annealing gains (in terms of superconductor J_c). Owing to sharpened cube texture and eliminated twinning, short-term annealing with its much higher throughput rate and lower cost is considered more advantageous. However, if sharpest texture is the goal, electropolishing of the very high temperature, long-term annealed tapes is an option to achieve smoothness. And an option for avoiding excessive grooving would be to follow a very short, very high temperature anneal with a lengthy soak at lower temperatures of 800-900°C.

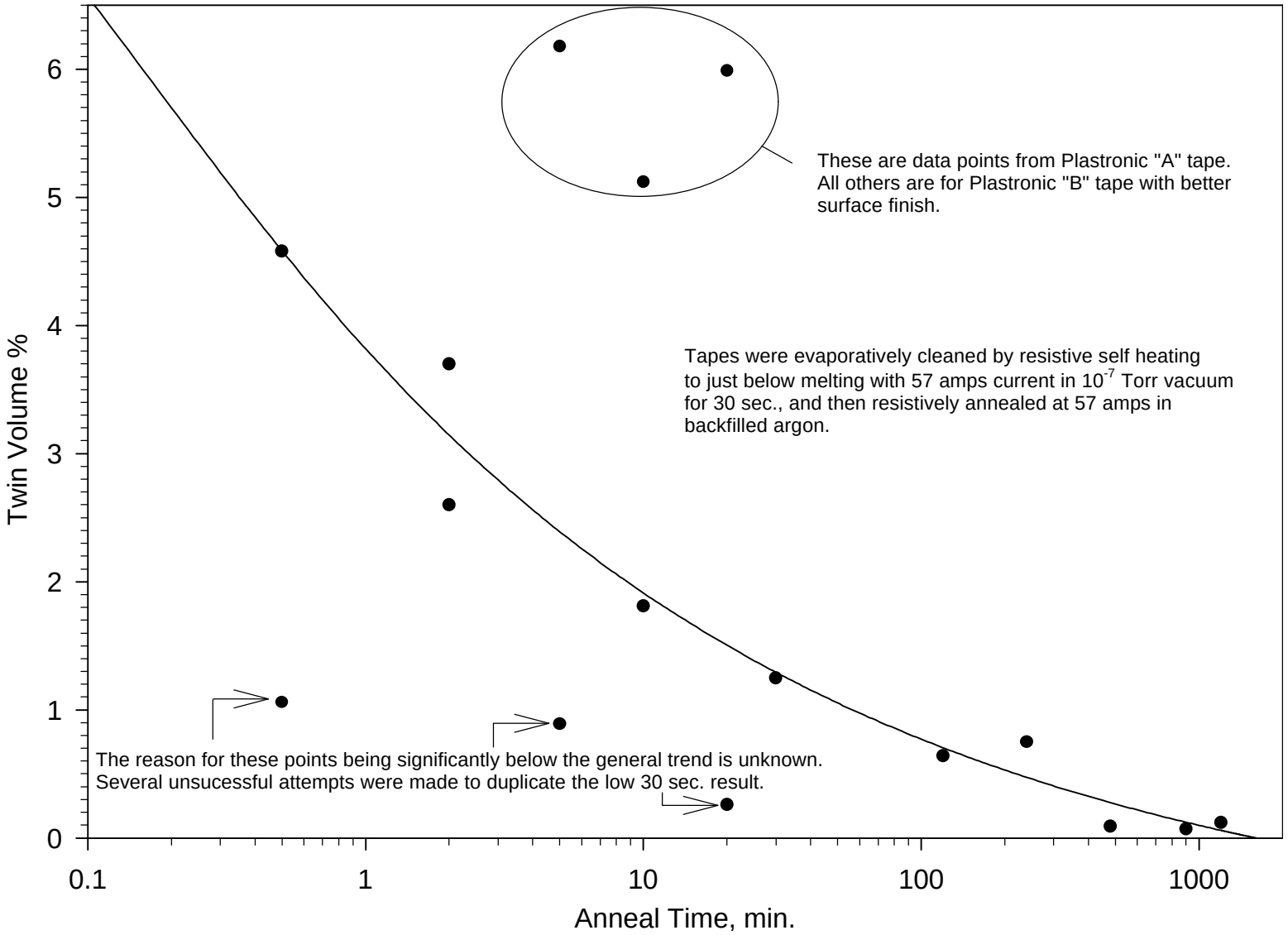

Figure 6.06-4. Effects of Anneal Time on Twinning in 99.98% Ni Tapes Annealed at Near the Melting Point.

OPEN ITEMS

A. UTSI:

None

B. DOE/FETC:

Awaiting review and approval for publication and distribution of Topical Report entitled, "*Evaluation of Methods for Application of Epitaxial Buffer and Superconductor Layer*s".

Awaiting review and approvals for manuscript entitled, *"Bench Scale Evaluation of Batch Mode Dip-Coating of Sol-Gel $LaAlO_3$ Buffer Material".*

Awaiting review and approval for publication and distribution of Topical Report entitled, *"Life Cycle Cost Study for Coated Conductor Manufacture by Electron Beam and Pulsed Laser Deposition Systems".*

Awaiting approval for the draft Quarterly Technical Progress Report for the period April 1, 1998-June 30, 1998 and July 2, 1998 through September 30, 1998.

Property Retirement Notices #15-#31 waiting processing and approval.

The Draft Management Plan covering the period October 1, 1998 through September 30, 1999 is awaiting approval by DOE.

SUMMARY STATUS ASSESSMENT AND FORECAST

Maintenance activities on the DOE facility were suspended throughout the quarter. Site environmental compliance was continued on a minimal basis with university funding. No work was performed on site environmental restoration. Government property accounting continued as required. DOE reporting activities continued as scheduled.

Work on the High Temperature Superconductor projects continued in accordance with the proposed management plan. Work on these projects is substantially on schedule except a report delayed due to illness of the researcher and a report on diagnostics delayed due to a management decision to add additional diagnostic technologies.

There are currently no tests scheduled in the CFFF. The Westinghouse Topping Combustor Test that was planned for the spring has been moved to AEDC. We continue efforts to find test programs that effectively utilize the facility.

TASK AND COST VARIANCES

The negative variances in Task 1 and charges to Tasks 2 and 3 reflect charges that were incurred in the previous quarter and entered into the accounting system after the stop work order on these tasks was issued.

The positive variance on Tasks 2 and 3 reflect an unexpended budget during the quarter for reporting and environmental activities in the proposed management plan due to the stop work order. The positive variance on Task 6 is small (4.7%) and indicative that expenditures are close to planned.

OCTOBER 1, 1998-DECEMBER 31, 1998 QUARTERLY VARIANCE REPORT

Planned vs. Actual Expenditures
(thousands of dollars)

TASK	PLANNED	ACTUALS	VARIANCE
1	0.0	30.6	-30.6
2	9.9	4.4	5.5
3	33.3	7.3	26.0
4	0.0	0.0	0.0
5	0.0	0.0	0.0
6	284.9	269.4	15.5
TOTALS	328.1	311.7	16.4
COST ELEMENT			
DIRECT LABOR	148.1	161.6	-13.5
FRINGE BENEFITS	31.6	32.8	-1.2
EQUIPMENT	34.4	9.6	24.8
EXPENDABLE MATERIAL	10.4	2.1	8.3
OUTSIDE CONTRACTS	4.8	5.5	-0.7
TRAVEL	5.0	3.8	1.2
TOTAL DIRECT COSTS	234.3	215.4	18.9
INDIRECT COSTS	93.8	96.3	-2.5
TOTAL	328.1	311.7	16.4

Planned vs. Authorized Funding
Cumulative

TASK	PLANNED	AUTHORIZED FUNDING
1	1496.4	
2	584.0	
3	476.7	
4	0.0	
5	0.0	
SUBTOTAL	2557.1	1982.7
6	3145.4	3355.8